PHYSICAL REVIEW E **70**, 055401(R) (2004)

# Deflagration-to-detonation transition in inertial-confinement-fusion baseline targets

P. Gauthier, F. Chaland, and L. Masse*
*Commissariat à l'Energie Atomique–Direction des Applications Militaires Île de France, Boîte Postale 12, 91680 Bruyères le Châtel, France*

(Received 4 December 2003; revised manuscript received 14 May 2004; published 11 November 2004)

By means of highly resolved one-dimensional hydrodynamics simulations, we provide an understanding of the burn process in inertial-confinement-fusion baseline targets. The cornerstone of the phenomenology of propagating burn in such laser-driven capsules is shown to be the transition from a slow unsteady reaction-diffusion regime of thermonuclear combustion (some sort of deflagration) to a fast detonative one. Remarkably, detonation initiation follows the slowing down of a shockless supersonic reaction wave driven by energy redeposition from the fusion products themselves. Such a route to detonation is specific to fusion plasmas.

DOI: 10.1103/PhysRevE.70.055401 PACS number(s): 52.57.−z, 47.40.−x

The initiation and propagation of self-sustained thermonuclear reaction waves is one of the most fundamental aspects of the physics of inertial-confinement fusion (ICF) using cryogenic deuterium and tritium (DT) spherical shells filled with DT gas. Although burn wave propagation under the central spark ignition scheme was openly discussed three decades ago [1] and, since then, has motivated a number of theoretical and numerical studies [2–5], to date a detailed evolutionary scenario of this combustion phase for ICF baseline targets is still missing. At the applied level, a better understanding of the burn process could be utilized to streamline the design of such targets and is a prerequisite to build relevant models.

In ICF, multiple shocks drive the capsule implosion [6] and finally initiate a central hot spot when penetrating, as a single shock, the low-density DT gas [7]. As compressive work from the incoming compressed outer shell makes the DT gas temperature and pressure elevate further, the hot spot mass gradually increases through continuous ablation of the inner part of the dense shell by electron thermal conduction (EC). One may anticipate that, once reactions are taking over from compressive work to heat the central part of the fuel, the accelerating ablation front transits in a continuous manner into a reaction-diffusion front (some sort of deflagration). However, our results reveal that the burn front is no longer deflagrative when sweeping the outer DT layers, but detonative: the bulk of the fuel appears to be ignited by a strong shock. The cornerstone of the phenomenology of the explosion of an ICF capsule is thus the transition from a slow (unsteady) reaction-diffusion regime of combustion to a fast reaction-compression one. This issue has received considerable attention in the field of chemical combustion [8–10] but also in the framework of supernova research [11,12]: only models of type Ia supernovae (SN Ia) in which a deflagration-to-detonation (DDT) occurs can account for the observed spectra and light curves [11,13]. However, to date, no agreement has been reached on the physical mechanisms by which a DDT may be initiated in thermonuclear systems such as SN Ia [11,12].

In this Rapid Communication, by means of highly resolved one-dimensional simulations, we provide an understanding of the burn process, from subsonic combustion to fast detonation, in ICF baseline capsules and, in doing this, we give a detailed description of a DDT in a fusion plasma. Detonation initiation is shown to follow the slowing down of a shockless supersonic reaction wave (RW) driven by energy redeposition from the combustion products themselves. Such a route to detonation differs from those so far exhibited in ordinary reactive gases [8–10] or speculated in SN Ia [11,12], which generally rely on the well-known Zel'dovich gradient mechanism [14,15] and require that prior to the onset of detonation the reactive medium has been preconditioned into a hot, spatially nonuniform state.

We emphasize that we have checked that the evolutionary scenario of the combustion phase we inferred is robust, i.e., rather insensitive to parameter or model variations. For instance, using the multigroup diffusion methods of [16] and [17], instead of solving numerically the time-dependent transport equation for the $\alpha$ particles, leaves the results unchanged. In fact, as discussed hereafter, only resorting to very crude approximations for describing energy redeposition from the fusion products (for example, assuming local energy deposition for the $\alpha$'s or the plasma thin to neutrons) has been found to significantly impact on the phenomenology of the DDT in ICF capsules.

The conventional ICF capsule we consider [18] consists of two concentric spherical shells with a low density inner DT gas fill. The outer shell is a 175-$\mu$m-thick Br-doped CH ablator and the inner shell is a 100-$\mu$m-thick cryogenic DT layer $[940 < R(\mu\mathrm{m}) < 1040]$, the mass of which is 310 $\mu$g. In such a system, the reaction $\mathrm{D}+\mathrm{T} \rightarrow \alpha(3.53\ \mathrm{MeV}) + n(14.05\ \mathrm{MeV})$ dominates. A shaped radiative temperature law [18], typical of the indirect drive geometry, is used to generate multiple shocks within the target. The maximum radiative temperature $T_r$ is adjusted so that the cryogenic DT maximum velocity is $V_{imp} = 3.87 \times 10^7$ cm/s. A detailed account of the stages of implosion, ignition, and combustion have been obtained from the one-dimensional Lagrangian code FCI1, described in detail elsewhere [19]. Specifically, for the simulations discussed at length in this paper, the time-dependent transport equation has been solved for the $\alpha$ particles.

*Email address: pascal.gauthier@cea.fr

 

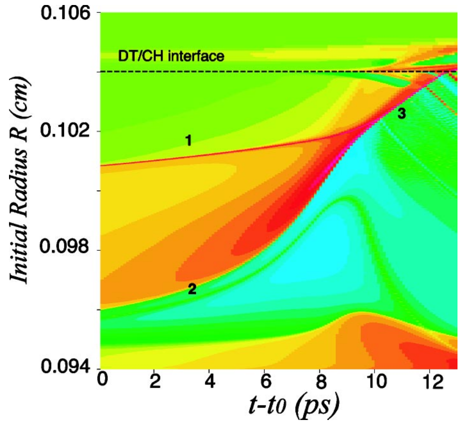


FIG. 1. (Color online) Time derivative of the density (arbitrary units) as a function of time and space. The DT gas is not represented. The figure shows the propagation of a variety of waves in the DT fuel, both compression (warm tints) and expansion waves (cold tints). The burn front, initially subsonic, will propagate in the most outer DT layers as a detonative igniting front (label 3). See the main text for further comments.

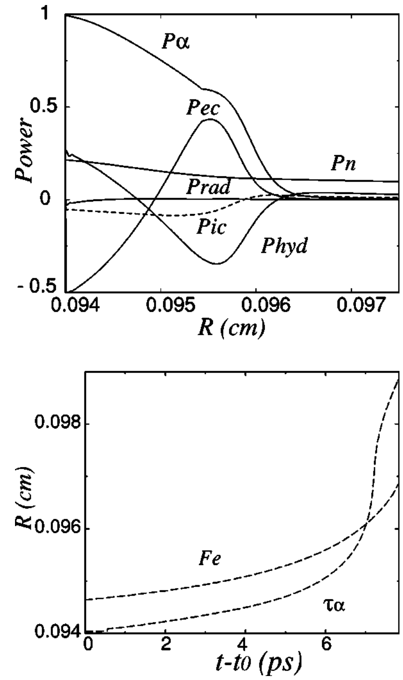


FIG. 2. (Top) Specific energy lost $(P<0)$ or gained $(P>0)$ by the plasma per units of time at $t=t_0+1.2$ ps as a function of space (Lagrangian coordinates). $P_\alpha$, $P_{rad}$, $P_{hyd}$, $P_{ec}$ $(P_{ic})$, and $P_n$ refer to contributions due to the $\alpha$ particles, radiation transfer, hydrodynamic work, electron (ion) thermal conduction, and neutrons. These quantities are normalized by the peak value of the $P_\alpha$ contribution at that time. (Bottom) Locus of positions of the peaks in reaction rate $\tau_\alpha$ and electron conduction flux $F_e$.

Figure 1 offers an overview of the stage of propagative burn. The reference time $t_0$ is defined as the instant at which 1% of the final output energy ($\simeq 34$ MJ) is released. In the following, all physical quantities are normalized by their peak value at $t_0$ (unless specified otherwise). Burn propagation is shown to last $t_{bp}\simeq 13$ ps. Prior to ignition, enhanced ablation by electron thermal conduction of the inner surface of the dense shell has produced a shock, which has caught at $t\simeq t_0-60$ ps the so-called reflected shock [7]. The shock wave resulting from this coalescence (label 1 in Fig. 1), seen to run ahead of the burn front (label 2) for $t-t_0<10$ ps, is of modest strength and responsible for only very weak thermonuclear activity.

Our numerical simulations indicate that for $t-t_0<5.5$ ps the burn front (label 2 in Fig. 1) is (i) traveling at subsonic speed relative to the upstream acoustic velocity, (ii) driven by thermal diffusion, and (iii) that the pressure variations across this front are much smaller than the corresponding changes in density and temperature. In reactive gaseous mixtures, conditions (i)–(iii) are typical of reaction-diffusion waves (i.e., deflagrations), the very specificity of the regime of propagative burn encountered here being its strong unsteadiness (see the discussion below). Figure 2 (top) indicates that radiation and ionic thermal conduction do not significantly contribute to the outward energy transfer. Although neutrons deposit some energy in the outer DT layers, outward propagation of the energy released by the reactions appears to be primary due to *both* remote energy deposition from the $\alpha$ particles and electron thermal conduction. In particular, in Fig. 2 (bottom) the RW path appears to remain strongly correlated with the EC wave path for $t-t_0<5.5$ ps. As it will become clear hereafter, this is because the fuel ahead of the region heated by the EC wave, not sufficiently preheated at these times by neutron energy deposition, is essentially thick to suprathermal ions. On the other hand, in ICF targets, one has $t_2\simeq t_{bp}\ll t_1$, where $t_1$ is the characteristic time of the thermonuclear reaction, $t_1=(n\langle\sigma V\rangle_{DT})^{-1}$, $n$ is the ionic density, and $t_2$ the characteristic time of burn wave development, $t_2\simeq 1/n\langle\sigma V\rangle_T[T_{peak}(\text{keV})/600]$, defined here as the time required for heating the DT fuel to the temperature $T_{peak}$ at which the Maxwellian plasma reactivity $\langle\sigma V\rangle_T$ peaks. This means that on the timescale $t_{bp}$ the reactions sharply intensify behind the combustion front which in turn gradually accelerates. This tends to compress the cold outer shell, as shown in Fig. 3. Under some circumstances [8,20], such a compression process induced by an accelerating thermal conduction wave culminates in the formation of a lead-

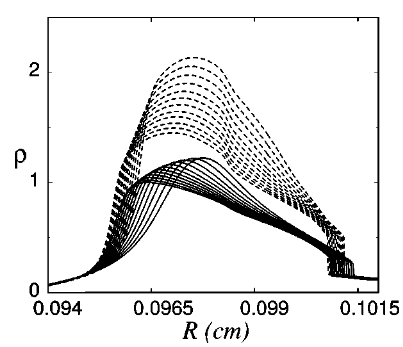


FIG. 3. Time evolution of the density spatial profile for $0<t-t_0(\text{ps})<5.5$ when plasma heating by neutrons is accounted for (solid lines) and neglected (dashed lines). All curves are normalized by the peak value of the density achieved at $t=t_0$ when neutron preheating is taken into account. Time step is $\Delta t=0.5$ ps.

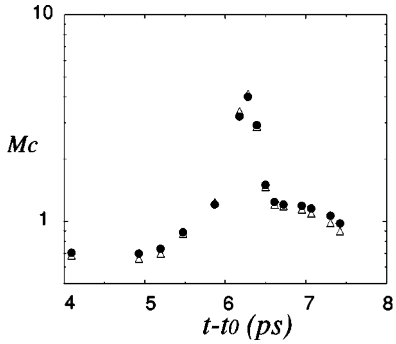


FIG. 4. Time evolution of the local Mach numbers of the reaction (•) and $\alpha$ (△) wave fronts.

ing shock wave that may (or may not) transit into a detonation. However, shock formation is hindered here since the compression process is limited in strength as a result of gradual preheating of the dense shell by neutron energy redeposition (Fig. 3).

For $t-t_0 \simeq 5.5$ ps, the burn regime suddenly changes, as seen in Fig. 2 (bottom): the RW appears to be strongly accelerated, its path being no longer correlated with the path of the EC wave. The explanation we provide on the basis of our detailed simulation is the following: as the reactions intensify, enhanced neutron energy redeposition in the outer shell promotes penetration of the suprathermal ions into these layers, the $\alpha$ particle range increasing for decreasing densities and increasing temperatures. Significant energy deposition from $\alpha$ particles then takes place ahead of those regions heated up by EC, i.e., in that part of the outer shell characterized by a sharp (positive) gradient in density $n$ (see Fig. 3). Reaction times $t_1$ ($\propto n^{-1}$), as well as characteristic times of burn wave development $t_2$ ($\propto t_1$), then strongly decrease and the $\alpha$ wave in turn accelerates when propagating up the density gradient. As long as the EC wave was crucial to promote the penetration of the suprathermal ions into the dense outer DT shell, the RW and EC wave paths (but also the $\alpha$ wave path) were strongly correlated and the RW was running at subsonic speed relative to the upstream medium. This is no longer true as the RW path becomes solely connected to the path of the leading $\alpha$ wave, whose speed appears to grow supersonic. As shown in Fig. 4, the process culminates in the triggering of a high-velocity (supersonic) shockless thermonuclear RW producing almost no mass motion and penetrating the dense shell. As long as the wave is traveling at supersonic speed relative both to the upstream and downstream acoustic velocity [for $5.5 < t-t_0(ps) < 7.3$], only weak intervention from hydrodynamics is expected. Subsequently, as the RW slows down past the local sound speed (deceleration starts as the reaction wave front reaches the top of the density profile), gasdynamics effects come into play: plasma expansion produces a shock wave [see Fig. 5 (top)], which amplifies during its propagation in the reactive medium and shortly transits into a detonative front (referred to as label 3 in Fig. 1). This latter appears to travel at a roughly constant speed in the most outer DT layers. In our simulation, 17 MJ are released during the whole stage of

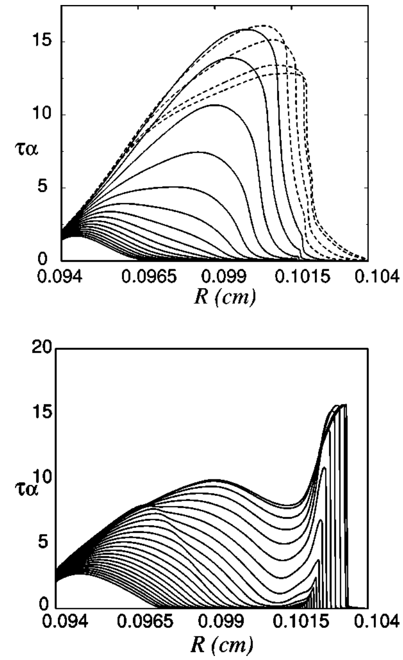


FIG. 5. Time evolution of the reaction rate spatial profile until detonation initiation (top) with and (bottom) without neutron preheating. The time step is $\Delta t = 0.3$ ps. The dashed lines are aimed at making visualization easier.

propagating burn and another 17 MJ is released in the stage of target disassembly that follows the transmission into the CH ablator of the detonation wave. On the other hand, only 2 MJ are delivered prior to the onset of the detonative regime of ignition.

It is worthwhile emphasizing that with a too crude treatment of $\alpha$ particle transport and/or neutron preheating one may miss some essential aspects of the evolutionary scenario described therein. For instance, one could argue that the plasma is essentially thin to energetic neutrons [21] and neglect neutron heating in the simulation. As seen in Fig. 3, the compression process ahead of the deflagrative-like burn front is then no longer hampered and culminates in the formation of a leading shock that causes secondary ignition in the upstream medium and detonation initiation [see Fig. 5 (bottom)]. According to our simulations, such a route to detonation is also encountered in the (unphysical) situation where neutron heating is accounted for but local energy deposition is assumed for the $\alpha$'s.

Such a detailed understanding of the burn process may shed light onto former ICF studies and can certainly be used to streamline target design. For instance, previous studies have shown that the result of increasing the initial gas fill density is to diminish the energy yield [21]. For the baseline ICF capsule considered in this Rapid Communication, our own simulations indicate that varying the initial fill density from 0.3 to 0.8 mg/cm$^3$ reduces the final energy release by about 25%. These results become comprehensible from the present analysis, once we have noticed that increasing the fill density also shortens the duration of the detonation stage

[22] whichturns out to be accompanied by much higher burn rates than the deflagrative one.

To conclude, accurate and well-resolved one-dimensional numerical computations have been carried on, providing an understanding of the burn process in baseline ICF targets. We have described the DDT in a thermonuclear plasma and demonstrated that, starting with an accelerating deflagrative-like burn front, a route to detonation specific to such media does exist.

We gratefully acknowledge stimulating discussions with P. Clavin and O. Larroche.

[1] H. N. Fisher *et al.*, Bull. Am. Phys. Soc. **18**, 683 (1973).
[2] G. S. Fraley *et al.*, Phys. Fluids **17**, 474 (1974).
[3] S. Yu. Gus'kov, O. N. Krokhin, V. B. Rozanov, Nucl. Fusion **16**, 957 (1976).
[4] V. V. Neudachin and P. V. Sasorov, Nucl. Fusion **33**, 475 (1993).
[5] R. Kishony, E. Waxman, and D. Shvarts, Phys. Plasmas **4**, 1385 (1997).
[6] A. Djaoui, Phys. Plasmas **3**, 4677 (1996).
[7] R. Betti *et al.*, Phys. Plasmas **8**, 5257 (2001).
[8] J. H. S. Lee and I. O. Moen, Prog. Energy Combust. Sci. **6**, 359 (1980).
[9] A. M. Bartenev and B. E. Gelfand, Prog. Energy Combust. Sci. **26**, 29 (2000).
[10] A. K. Kapila *et al.*, Combust. Theory Modell. **6**, 553 (2002).
[11] A. M. Kolkhlov, E. S. Oran, and J. C. Wheeler, Astrophys. J. **478**, 678 (1997).
[12] J. C. Niemeyer, Astrophys. J. **523**, L57 (1999).
[13] P. Höflich, A. M. Kolkhlov, and J. C. Wheeler, Astrophys. J. **444**, 831 (1995).
[14] Ya. B. Zel'dovich *et al.*, Acta Astron. **15**, 313 (1970).
[15] Ya. B. Zel'dovich, Combust. Flame **39**, 211 (1980).
[16] J. P. Morreeuw, C. R. Seances Acad. Sci., Ser. 2 **293**, 1021 (1981).
[17] E. G. Corman *et al.*, Nucl. Fusion **15**, 377 (1975).
[18] P. A. Holstein *et al.*, C. R. Acad. Sci., Ser IV: Phys., Astrophys. **1**, 693 (2000).
[19] D. Besnard, G. Bonnaud, and G. Schurtz, in *La Fusion Themonucléaire par Laser*, edited by R. Dautray and J. P. Watteau (Eyrolles, Paris, 1993), Part 3, Vol. 2, Chap. 13.
[20] V. Kurdyumov, A. L. Sanchez, and A. Linan, J. Fluid Mech. **491**, 379 (2003).
[21] J. D. Lindl, Phys. Plasmas **11**, 339 (2004).
[22] L. Masse *et al.*, Phys. Plasmas (to be published).